

NON INTRUSIVE 3D LOAD CALCULATION DURING YAW CONDITIONS

Vanessa del Campo

UPC (ETSEIAT)

Vanessa.del.Campo@upc.edu

Daniele Ragni

TUDeft (DUWIND)

D.Ragni@tudelft.nl

Daniel Micallef

TUDeft (DUWIND)

D.Micallef@tudelft.nl

Busra Akay

TUDeft (DUWIND)

B.Akay@tudelft.nl

Javier Diez

Rutgers University

diez@jove.rutgers.edu

Carlos Simao Ferreira

TUDeft (DUWIND)

C.J.SimaoFerreira@tudelft.nl

Abstract

The blade of a scaled down Horizontal Axis Wind Turbine working in Yawed Flow conditions has been investigated by means of Stereoscopic Particle Image Velocimetry. The goal was to obtain, simultaneously, the 3D velocity field surrounding the blade, the pressure distribution around it and the aerodynamic loads being exerted on the blade, responsible for thrust and torque.

Keywords: PIV, blade loading, aerodynamics, pressure reconstruction, yaw.

1. Introduction

The method presented allows the designer to calculate forces on Horizontal Axis Wind Turbine (HAWT) blade with a non intrusive technique. Thus, it eliminates the need of modifying the model by introducing pressure tabs, which are difficult to implement on a rotating machine [9] and, in some cases where the model is small, unfeasible.

With this technique, it is possible to calculate loads in any chosen position of the blade, obtaining, in addition, information on the 3D flow around the section which is under study.

Furthermore, the fact of operating the HAWT in a 30° yawed flow introduces azimuthal asymmetry and imposes an unsteady condition in the mathematical approach. This allows measuring forces on the HAWT also when it is operating out of its design working conditions.

In the last years, there have been several studies that proved the feasibility of calculating fluid dynamic loads using only velocity fields and their derivatives. One of the first considerations was undertaken by Unal et al. [11], who calculated force coefficients on a cylinder. In parallel, Noca et al. [6] developed a way of calculating loads on a bluff body without the need of explicitly evaluating the pressure term, using a vorticity based approach of the Momentum Equation. More recently, other research groups have tackled the subject; Kurtulus et al. [5] measured unsteady forces on a cylinder, van Oudheusden et al. [7] evaluated forces for compressible flows on a transonic airfoil, and Ragni et al. [8] analyzed the aerodynamic loads on an aircraft propeller blade with axial flow.

2. Experimental Apparatus and Procedure

The experimental campaign presented herein was performed at the Open Jet Facility (OJF) at TUDeft. The closed circuit

wind tunnel has an octagonal jet exit equivalent to a 3 m diameter and the size of the test section is 6 x 6.5 x 13.5 m³, as shown in Figure 1. The flow velocity was fixed to 6 m/s.

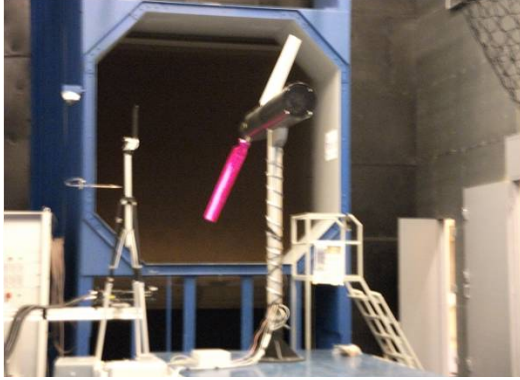


Figure 1: OJF Experimental Campaign

The HAWT model tested was composed of 2 blades and had a total radius of $R = 1\text{m}$. It was operated by an electrical engine that turned it at a constant angular velocity of 400 rpm. The airfoil section used all along the blade was a DU-96-W180. The blade was not pitched but it was tapered and twisted. The HAWT model was placed with its rotation axis displaced 30° from the tunnel flow, so as to reproduce yaw conditions. Table 1 summarizes the experimental conditions and Figure 2 depicts the set up used.

Experimental Conditions	
Yawed Flow (30°)	6 m/s
Angular Velocity	400 rpm
Room Temperature	21°
Atmospheric Pressure	101050 Pa
Blade Geometry	DU-96_W180
Maximum Twist (tip)	-15°

Table 1: Experimental Conditions

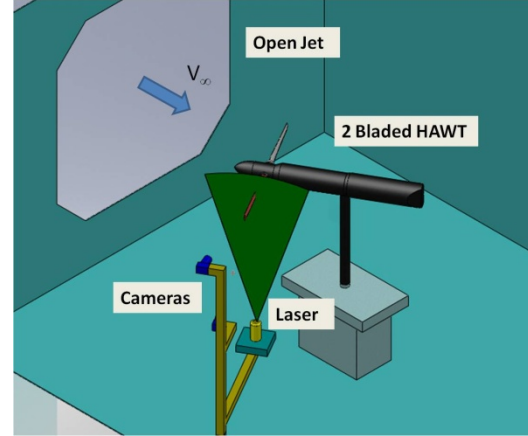


Figure 2: Yaw Conditions Set Up

In order to acquire 3D velocity information around the blade, 30 span sections were studied for three different time steps: when the blade was exactly at 90° azimuth, and also when the blade was near and passed this position, in order to have time-dependent information. For each phase-locked velocity plane 100 SPIV images were obtained.

Both the two cameras and the laser were mounted in a computerized traverse system. This was very convenient since it made it unnecessary to redo the calibration for each radial position. Table 2 presents main SPIV imaging and acquisition parameters.

Particle Image Velocimetry Parameters	
Laser Type	Double pulsed NdYAG (300mJ)
Seeding	Diethylene Glycol and Water
Particle Diameter	$1\mu\text{m}$ (median)
Camera Resolution	$4830 \times 3230\text{px}^2$
Focal Length	180mm
Diaphragm Aperture	5.6
Field of View	$250 \times 220\text{mm}^2$
InterrogationWindow	32×32 (50% overlap)
Spatial Resolution	1.8mm

Table 2: SPIV Imaging and Acquisition Parameters

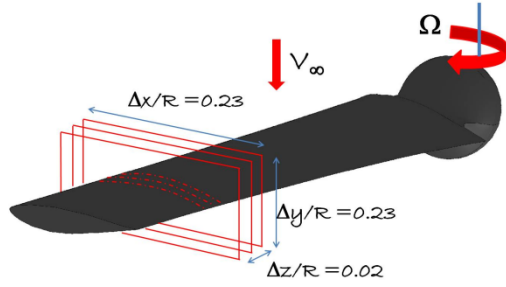


Figure 3: Control Volume Approach

Aerodynamic loads were calculated with a 3D approach using the velocity data obtained with SPIV. This was done by measuring the change in momentum of the flow inside a finite control volume surrounding the airfoil, as it expressed in Equation (1). The control volume should have no other external forces apart from those caused by the blade element itself [2]. Figure 3 represents the control volume chosen for the calculation.

$$\vec{F} = - \underbrace{\iint p \vec{n} ds}_{\text{Pressure terms}} + \underbrace{\iint \vec{\tau} \vec{n} ds}_{\text{Viscous terms}} - \underbrace{\frac{d}{dt} \iiint \rho \vec{V} dv}_{\text{Local accel.}} - \underbrace{\iint \rho (\vec{V} \vec{n}) \vec{V} ds}_{\text{Convective accel.}} - \underbrace{\iiint 2\rho (\vec{\Omega} \times \vec{V}) dv}_{\text{Coriolis accel.}} - \underbrace{\iiint \rho (\vec{\Omega} \times (\vec{\Omega} \times \vec{r})) dv}_{\text{Centrifugal accel.}} \quad (1)$$

If a moving frame of reference was chosen (placed in the rotating blade), non inertial terms had to be taken into account, whereas these terms were not necessary if a stationary frame of reference was considered. Reynolds Stress Terms were considered in the formulation as well. Finally, since the flow encountered by the blade while rotating changes with azimuth, unsteady terms were also included in the 3D formulation, regardless of the frame of reference chosen.

The pressure gradient was derived from the momentum equation in its differential form, as it is shown in Equation (2).

$$\vec{\nabla} p = - \underbrace{\frac{d}{dt} (\rho \vec{V})}_{\text{Local accel.}} - \underbrace{\rho \vec{V} \cdot \vec{\nabla} \vec{V}}_{\text{Convective accel.}} + \underbrace{2\rho (\vec{\Omega} \times \vec{V})}_{\text{Coriolis accel.}} + \underbrace{\rho (\vec{\Omega} \times (\vec{\Omega} \times \vec{r}))}_{\text{Centrifugal accel.}} + \underbrace{\mu \Delta \vec{V}}_{\text{Visc. stress}} \quad (2)$$

Thus, the pressure terms were calculated solving the Poisson Pressure Equation (see Equation (3)) in all the flow field, using a forcing function $g(u, v)$ which is derived from the velocity field itself using the Momentum Equation. The discretization of the Laplace operator is done using finite differences, which provides with matrix D .

$$\Delta p \approx Dp = g(u, v) \rightarrow D^{-1}g(u, v) \quad (3)$$

With the aim of comparing the results obtained experimentally, a computational panel method was used to simulate the HAWT working in the same conditions. The model used was developed by Dixon [3] following the formulation presented by Katz and Plotkin [4] and validated by Simao Ferreira [10]. It is a 3D model that assumes potential flow and can represent multibody, unsteady problems.

3. Results

Tangential and Normal forces were calculated per unit length at 10 different span positions of the rotating blade, at a 30° yaw condition. Velocity fields were concurrently obtained, an example of which might be seen in Figure 4, which depicts absolute velocities that would be used with a stationary frame of reference formulation. Figure 5 depicts relative velocities of the

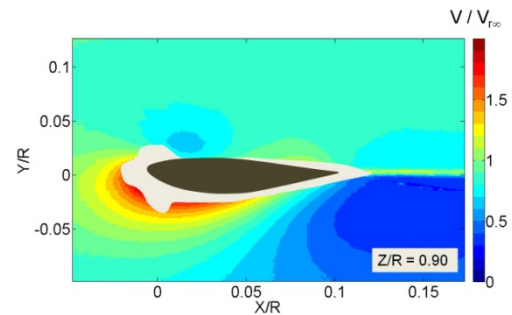


Figure 4: Absolute Velocity at $z/R = 0.9$

same blade span position, as would be used in a moving frame of reference formulation. The reflections of the laser light hindered having a good PIV image quality in the regions close to the airfoil and forced to mask this region.

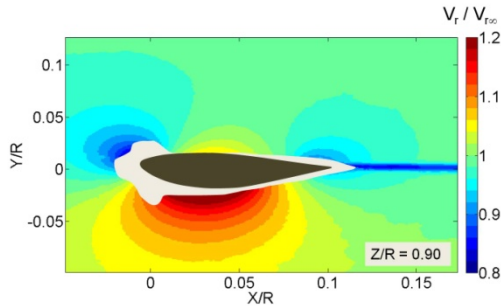


Figure 5: Relative Velocity at $z/R=0.9$

The pressure reconstructed using the Poisson Pressure Solver is depicted in

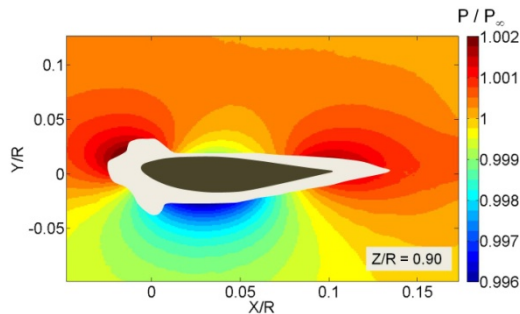


Figure 6: Poisson Pressure Reconstruction

Figure 6. This method does not assume an irrotational flow, and thus, the results differ from the pressure field that would be calculated using just the Bernoulli Theorem (which is depicted in Figure 7), specially in the wake region, where the vorticity is bigger.

Final load calculation results are shown in Figure 8 and Figure 10, both for a moving frame of reference (m.f.r) and a stationary frame of reference (s.f.r). PIV Normal force calculations are very similar regardless of the frame of reference chosen, and show the same tendency as the Panel Code results, although there is a small offset of the 10% of the total in the regions near the tip. The PIV-Loads code was previously validated with DNS data [1], giving exact results. The difference encountered with the Panel Code results are due to:

- a) PIV uncertainties: mainly peak locking, lack of spatial resolution in the wake and laser reflections.
- b) Panel Code assumptions leading to lack of accuracy in its predictions.

Figure 9 shows the different contributions of the Momentum Equation terms to the final normal force calculation at a given span position. Unsteady terms and pressure terms are the most important when using a stationary frame of reference, whereas convective and pressure terms are predominant when using a moving frame of reference.

Tangential forces calculated with PIV are more random, since the wake region here is playing an important role, and in this area PIV uncertainties are larger. Figure 10 shows the Normal Force calculation, concluding that, using a stationary frame of reference in which the volume integrals have been transformed into surface integrals (following the method proposed by Wu et al. [12]), brings more accurate results.

Finally, Figure 11 decomposes the Momentum Equation contributions to the final Tangential Force calculation.

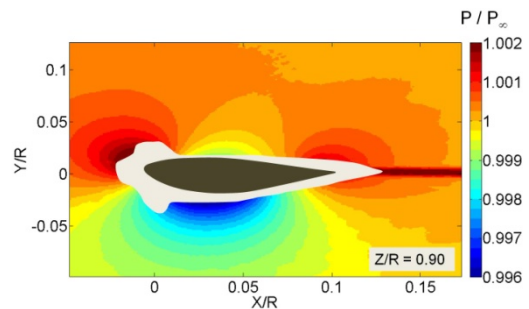


Figure 7: Bernoulli Pressure Reconstruction

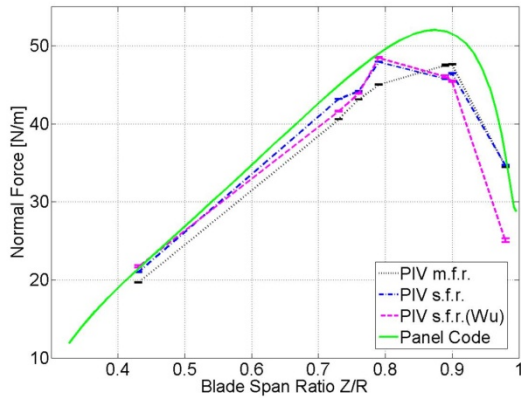


Figure 8: Normal Force Calculations

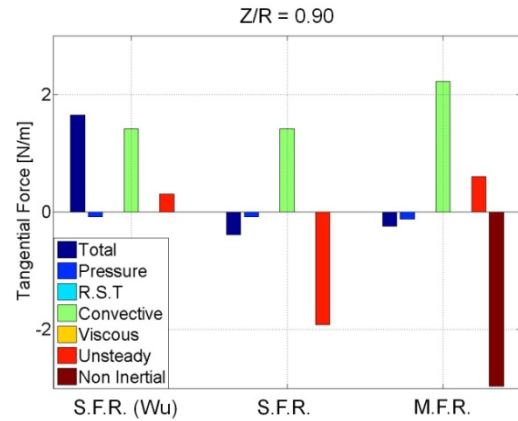


Figure 11: Momentum Equation Contributions to the Tangential Force Calculations (see Equation (2))

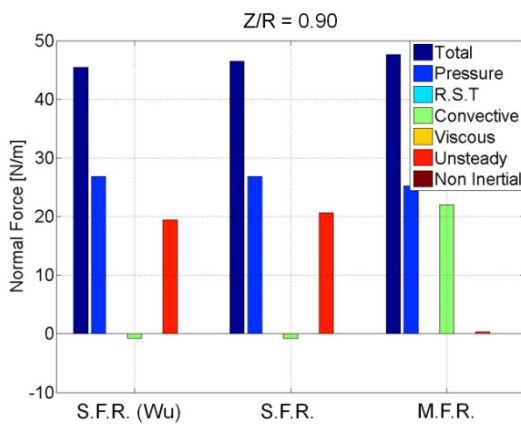


Figure 9: Momentum Equation Contributions to the Normal Force Calculations (see Equation (2))

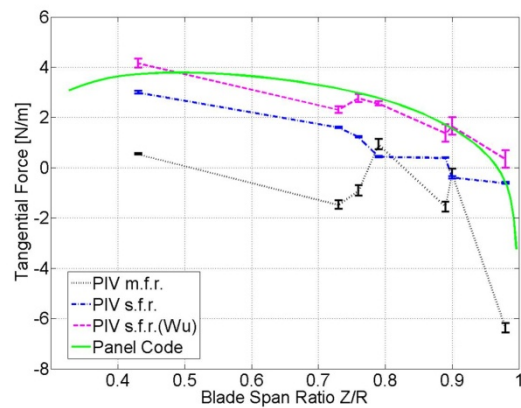


Figure 10: Tangential Force Calculations

4. Conclusions

A non-intrusive technique to calculate loads in a HAWT, based in SPIV, has been investigated. Aerodynamic loads have been measured in a rotating HAWT blade working in Yaw conditions. This leads to a non-steady formulation, even if a moving frame of reference is chosen. For each sectional plane investigated, 5 phase-locked 3D velocity planes are needed (3 different time steps, 3 different span positions).

The results show good agreement with Panel Code results regarding Normal Forces. However, a bigger randomness is encountered when studying Tangential Forces. Future improvements in SPIV resolution and implementations will certainly lead to better results.

The technique, which does not require the modification of the model, brings new possibilities of studying the Aerodynamics of Small Wind Turbines and the effectiveness of Active Load Control Methods. It also allows the designer to focus the experimental investigation in any particular Span Position of the blade whose Aerodynamic Performance needs to be improved or revised.

References

- [1]. T. Albrecht, J. Stiller. Control of Separated Flow Using an Oscillating Lorentz Force: Comparison of DNS, LES, and Experiments. *Progress in Turbulence III 2009*.
- [2]. J.D. Anderson. Fundamentals of aerodynamics. *McGraw-Hill New York 2001*.
- [3]. K. Dixon. The near wake structure of a vertical axis wind turbine. *Masters thesis, Technische Universiteit Delft, The Netherlands 2008*.
- [4]. J. Katz, A. Plotkin. Low-speed aerodynamics. *Cambridge University Press, Cambridge 2001*.
- [5]. D.F. Kurtulus, F. Scarano and L. David. Unsteady aerodynamic forces estimation on a square cylinder by TR-PIV. *Experiments in fluids 2007*.
- [6]. F. Noca, D. Shiels and D. Jeon. A comparison of methods for evaluating time-dependent fluid dynamic forces on bodies, using only velocity fields and their derivatives. *Journal of Fluids and Structures 1999*.
- [7]. B.W. van Oudheusden, F. Scarano, E.W.M. Roosenboom, E.W.F. Casimiri, and L.J. Souverein. Evaluation of integral forces and pressure fields from planar velocimetry data for incompressible and compressible flows. *Experiments in Fluids 2007*.
- [8]. D. Ragni, B.W. van Oudheusden and F. Scarano. 3D pressure imaging of an aircraft propeller blade-tip flow by phase-locked stereoscopic PIV. *Experiments in fluids 2012*.
- [9]. S. Schreck, T. Sant and D. Micallef. Rotational augmentation disparities in the mexico and uae phase vi experiments. *3rd Torque 2010 The Science of making Torque from Wind Conference (FORTH, Heraklion, Crete, Greece)*.
- [10]. C.J. Simao Ferreira. The near wake of the VAWT: 2D and 3D views of the VAWT aerodynamics. *PhD Thesis, Technische Universiteit Delft, The Netherlands 2009*
- [11]. M.F. Unal, J.C. Lin and D. Rockwell. Force prediction by PIV imaging: a momentum-based approach. *Journal of fluids and structures 1997*.
- [12] J. Wu, L. Chen, and Z. Shi. Particle image velocimetry (PIV) measurements of tip vortex wake structure of wind turbine. *Applied Mathematics and Mechanics, 2011*.